

ARTICLE TYPE

Probabilistic performance validation of deep learning-based robust NMPC controllers

Benjamin Karg¹ | Teodoro Alamo² | Sergio Lucia^{*1}

¹Chair of Internet of Things for Smart Buildings, Technische Universität Berlin and Einstein Center Digital Future, Einsteinufer 17, 10587 Berlin Germany

²Departamento de Ingeniería de sistemas y Automática, Universidad de Sevilla, Escuela Superior de Ingenieros, Camino de los Descubrimientos s/n, 41092 Sevilla, Spain

Correspondence

*Corresponding author Sergio Lucia. Email: sergio.lucia@tu-berlin.de

Summary

Solving nonlinear model predictive control problems in real time is still an important challenge despite of recent advances in computing hardware, optimization algorithms and tailored implementations. This challenge is even greater when uncertainty is present due to disturbances, unknown parameters or measurement and estimation errors. To enable the application of advanced control schemes to fast systems and on low-cost embedded hardware, we propose to approximate a robust nonlinear model controller using deep learning and to verify its quality using a posteriori probabilistic validation techniques.

We use a probabilistic validation technique based on finite families, combined with the idea of generalized maximum and constraint backoff to enable statistically valid conclusions related to general performance indicators. The potential of the proposed approach is demonstrated with simulation results of an uncertain nonlinear system.

KEYWORDS:

model predictive control, robust control, probabilistic validation, machine learning

1 | INTRODUCTION

Model predictive control is a popular advanced control technique that can deal with nonlinear systems and constraints while considering general control goals that go beyond conventional set-point tracking tasks. Two of the main obstacles that one faces when implementing and designing a nonlinear model predictive controller are the accuracy of the model and the computational complexity needed to solve a non-convex optimization problem online, which often renders its implementation too slow for fast systems or impossible to be deployed on resource-constrained embedded platforms.

Handling uncertainty in the context of model predictive control is the main goal of robust MPC. Traditional min-max approaches [1] do not explicitly consider the fact that new information will be available in the future, which leads to over-conservative solutions. Closed-loop robust MPC avoids the problem of conservativeness by optimizing over control policies instead of optimizing over control inputs [2], leading however to intractable formulations in the general case. Most of the recent robust MPC methods focus on achieving a good trade-off between complexity and performance. Tube-based approaches [3] decompose the robust MPC problem into a nominal MPC and an ancillary controller. The ancillary controller makes sure that the real uncertain system stays close to the trajectory planned by the nominal MPC. By tightening the constraints of the nominal MPC, robust constraint satisfaction can be achieved. In the simplest version, the complexity of tube-based MPC is the same as that of standard MPC. However, if an increased performance is desired, the complexity grows as presented in [4] or [5]. Scenario tree-based [6, 7, 8] or multi-stage MPC [9] represents the evolution of the uncertainty using a tree of discrete uncertainty realizations. An improved performance can be often seen in practice [10] because the feedback structure is not restricted to be affine,

as usually done in tube-based MPC and in other robust approaches [11]. While it is also possible to achieve stability and robust constraint satisfaction guarantees for a multi-stage MPC formulation [7, 12], but its computational complexity grows exponentially with the number of uncertainties. The presence of uncertainty significantly increases the computational complexity of any NMPC implementation if a non-conservative performance is desired.

The last decade has witnessed an important progress on hardware, algorithms and tailored implementations that enable the efficient solution and implementation of NMPC controllers based, for example, on code generation tools [13, 14] that provide efficient implementations of linear and nonlinear MPC on embedded hardware, including low-cost microcontrollers [15] and high-performance FPGAs [16].

A different possibility to achieve embedded nonlinear model predictive control is the use of approximate explicit nonlinear model predictive control [17, 18] based on approximating the multi-parametric nonlinear program using similar ideas as for explicit MPC of linear systems [19]. We propose in this work to use deep neural networks to approximate a robust multi-stage NMPC control law. The idea of using a neural network as function approximator for an NMPC feedback law was already proposed by [20] back in 1995, but only very recently [21, 22] deep neural networks (neural networks with several hidden layers) have been proposed as function approximators. The use of deep neural networks is motivated by recent theoretical results that suggest the exponentially better approximation capabilities of deep neural networks in comparison to shallow networks [23].

Assessing the closed-loop performance of approximate controllers, or any other controller subject to further random disturbances or estimation errors, is particularly challenging in the case of complex nonlinear systems. The theory of randomized algorithms [24], [25] provides different schemes capable of addressing this issue. For example, statistical learning techniques can be used to design stochastic model predictive controllers with probabilistic guarantees [26], [27], [28]. Also, under a convexity assumption, convex scenario approaches [29] can be used in the context of chance constrained MPC [30], [31], [32]. The main limitation of the aforementioned approaches based on statistical learning results [24], [33] and scenario based ones [29] is that the number of random scenarios that have to be generated (sample complexity), grows with the dimension of the problem.

Probabilistic validation [34], [35], allows one to determine if a given controller satisfies, with a prespecified probability of violation and confidence, the control constraints. The sample complexity in this case does not depend on the dimension of the problem, but only of the required guaranteed probability of violation and confidence. Examples of probabilistic verification approaches in the context of control of nonlinear uncertain systems can be found, for example, in [25], [36] and [37]. These techniques have also been used for the probabilistic certification of the behaviour of off-line approximations of nonlinear control laws [38], [39].

The main contribution of this paper, which extends the results from [40], is the formulation of general closed-loop performance indicators that are not restricted to binary functions as in [38] and can be computed simulating the closed-loop system with any given controller. We also provide sample complexity bounds that do not grow with the size of the problem for the case of a finite family of design parameters and general performance indicators. Our approach allows to discard a finite number of worst-case closed-loop simulations, improving significantly the applicability of the probabilistic validation scheme compared to existing works. The potential of the presented approach is illustrated for a highly nonlinear towing kite system including a real-time capable embedded implementation of an approximate, but probabilistically safe, robust nonlinear model predictive controller on a low-cost microcontroller.

The paper is organized as follows. Section 2 includes the mathematical framework for the output feedback robust NMPC problem considered in this work. The use of deep learning to obtain approximate robust NMPC controllers is summarized in Section 3 while the introduction of several closed-loop performance indicators is included in Section 4. A novel probabilistic validation methodology is presented in Section 5. The case study is detailed in Section 6, the results in Section 7 and the paper is concluded in Section 8.

2 | ROBUST OUTPUT-FEEDBACK NONLINEAR MODEL PREDICTIVE CONTROL

We are interested in optimally controlling the following nonlinear discrete time system:

$$x(k+1) = f(x(k), u(k), d(k)), \quad (1)$$

$$y(k) = h(x(k), u(k), d(k)), \quad (2)$$

where $x(k) \in \mathcal{R}^{n_x}$ is the state vector, $u(k) \in \mathcal{R}^{n_u}$ is the control input, and $d(k) \in \mathcal{R}^{n_d}$ is the disturbance vector. In general, not all states can be measured, and a state estimate $\hat{x}(k)$ should be computed based on the past measurements $y(k) \in \mathcal{R}^{n_y}$. It is assumed that the disturbances $d(k)$ take values, with high probability, from a known set \mathcal{D} .

The closed-loop trajectory should satisfy general nonlinear input and state constraints defined by

$$g_l(x(k), u(k), d(k)) \leq 0, \quad l = 1, \dots, n_g, \quad (3)$$

where n_g is the number of constraints. Robust MPC schemes have four important characteristics that differentiate one approach from the other: The choice of cost function; The propagation of the uncertainty; Robust constraint satisfaction; The characterization of feedback information.

The *cost function* can be chosen following a min-max approach, where the worst-case realization of the uncertainty $d(k)$ at each step in the prediction is chosen [1]. Tube-based methods usually choose the cost incurred by the closed-loop system driven by the nominal realization of the uncertainty [41]. Scenario-tree based methods use a weighted sum of a set of discrete scenarios [9] and stochastic MPC schemes [7] make use of, e.g., the expectation operator. In this work, we consider a general cost function $V_D(N_p, \hat{x}(0))$ that depends on the current estimate of the states $\hat{x}(0)$ and the prediction horizon N_p .

The *propagation of the uncertainty* is one of the key elements of any robust NMPC scheme. A general framework, which is used in this work, is the definition of reachable sets at each sampling time in the prediction based on a current initial condition, the system model, the applied input and the uncertainty set \mathcal{D} . The reachable set at sampling time $k+1$ can be thus denoted as:

$$\mathcal{X}(k+1) = \{f(x(k), u(k), d(k)) : x(k) \in \mathcal{X}(k), d(k) \in \mathcal{D}\}. \quad (4)$$

There are several methods to compute such reachable sets. In the linear case, the consideration of the vertices of the uncertain set and their propagation along the prediction horizon is enough to compute an exact reachable set. In the nonlinear case, linearization techniques [42] or ODE bounding techniques [43] can be used to obtain guaranteed over-approximations, which can be then used in robust optimal control schemes. To maintain the notation independent of the method used to obtain an (over-) approximation of the reachable sets at each sampling time, the *bounding* operators denoted as $\diamond f(\cdot)$ are used, which are defined as:

$$\mathcal{X}(k+1) = \diamond f(\mathcal{X}(k), u(k), \mathcal{D}). \quad (5)$$

Another possibility for the propagation of uncertainty is to resort to probabilistic reachable sets as done in [44].

Robust constraint satisfaction is often one of the main motivations for the use of a robust NMPC approach. It means that the requirements of the closed-loop system in form of input and state constraints should be satisfied for all possible outcomes of the uncertainty and it is usually enforced by embedding the reachable sets into the constraints of an optimization problem.

The *characterization of feedback* that is employed is another key property of any robust MPC scheme. It is well known that considering a sequence of optimal control inputs in the prediction under uncertainty can result in very conservative performance of the closed-loop because it is ignored that new information about the future will be available in the form of measurements and thus future actions can be adapted accordingly. To avoid this conservatism, closed-loop approaches can be used, in which one optimizes over a sequence of control policies μ and can be formulated as the receding horizon solution of the following optimization problem:

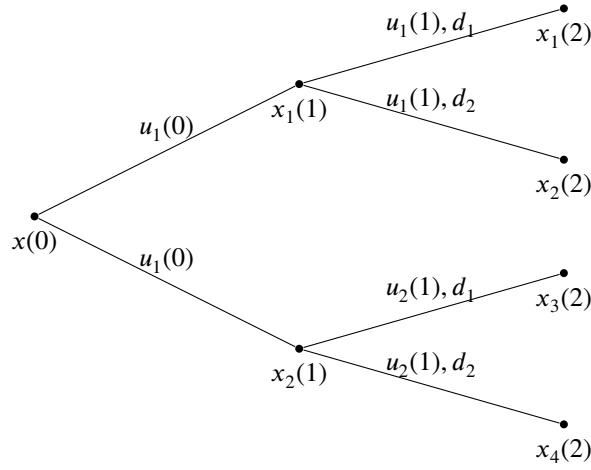
$$\underset{\mu(\cdot)}{\text{minimize}} \quad V_D(N_p, \hat{x}(0)), \quad (6a)$$

$$\mathbb{P}_{\text{ideal}} : \quad \text{subject to} \quad \mathcal{X}(k+1) = \diamond f(\mathcal{X}(k), \mu(\mathcal{X}(k)), \mathcal{D}), \quad \text{for } k = 0, \dots, N_p - 1, \quad (6b)$$

$$g_l(\mathcal{X}(k), \mu(\mathcal{X}(k)), \mathcal{D}) \leq 0, \quad l = 1, \dots, n_g, \quad \text{for } k = 0, \dots, N_p - 1, \quad (6c)$$

$$\mathcal{X}(N_p) \subseteq \mathcal{X}_f, \quad (6d)$$

$$\mathcal{X}(0) = \{\hat{x}(0)\} \oplus \mathcal{E}_{\text{est}}, \quad (6e)$$



$$\tilde{\mathcal{X}}(0) = \{x(0)\}; \quad \tilde{\mathcal{X}}(1) = \{x_1(1), x_2(1)\}; \quad \tilde{\mathcal{X}}(2) = \{x_1(2), \dots, x_4(2)\};$$

FIGURE 1 Scenario tree representation.

where the constraints (6c) denote that $g_l(x, \mu(x), d) \leq 0$ should be satisfied for all $x \in \mathcal{X}(k)$ and for all $d \in \mathcal{D}$.

Solving the ideal robust NMPC problem $\mathbb{P}_{\text{ideal}}$ defined in (6), one obtains a receding horizon policy $\kappa_{\text{ideal}}(\hat{x}(0))$ which is a function of the initial state estimate $\hat{x}(0)$ that has been obtained with a certain estimation error bounded by \mathcal{E}_{est} .

Obtaining an exact solution of $\mathbb{P}_{\text{ideal}}$ is usually intractable mainly because of the bounding operator $\diamond f(\cdot)$ and the general feedback law $\mu(\cdot)$. There are different alternative solutions to obtain approximations of this problem. A common simplifying assumption is to restrict the search to affine policies on the state or on the disturbances [11]. A different alternative is the use of a scenario tree [6], [7], [9] in a so-called multi-stage NMPC approach. A multi-stage NMPC scheme is based on the representation of the uncertainty via a scenario tree (see Figure 1), which branches at each sampling time. This means that the uncertainty set is approximated by a discrete number of uncertainty realizations:

$$\mathcal{D} \approx \tilde{\mathcal{D}} = \{d_1, \dots, d_s\} \quad (7)$$

where s is the number of possible realizations of the uncertainty that are considered in the tree. Using a scenario tree formulation, an approximation of the reachable set can be obtained as the convex hull of the set of all the nodes at a given stage, i.e.:

$$\mathcal{X}(k) \approx \text{Conv}(\tilde{\mathcal{X}}(k)) = \text{Conv}\left(\bigcup_{i=1}^{s^k} x_i(k)\right), \quad (8)$$

where $\text{Conv}(\cdot)$ denotes the convex hull of a set and $x_i(k)$ denotes the node i of the tree at stage k as depicted in Figure 1. In the linear case with polytopic uncertainty, including the extreme values of the uncertainty in $\tilde{\mathcal{D}}$ guarantees an exact representation of the actual reachable set. In the nonlinear case considered in this paper it is only an approximation and therefore we focus on the point-wise approximation $\tilde{\mathcal{X}}$. Following the same notation, the bounding operator used to propagate the point-wise uncertainty description can be denoted as:

$$\tilde{\mathcal{X}}(k+1) = \diamond f(\tilde{\mathcal{X}}(k), \mu(\tilde{\mathcal{X}}(k)), \tilde{\mathcal{D}}) \approx \bigcup_{i=1}^{s^k} \bigcup_{j=1}^s f(x_i(k), u_i(k), d_j). \quad (9)$$

The cost function is usually chosen as a weighted sum of the stage cost for each node in the scenario tree:

$$V_D(N_p, \hat{x}(0)) = \sum_{k=0}^{N_p-1} \sum_{i=1}^{s^k} \ell(x_i(k), u_i(k)) + \sum_{i=1}^{s^{N_p}} V_f(x_i(N_p)). \quad (10)$$

Introducing (10) and (9) in the ideal formulation of robust NMPC $\mathbb{P}_{\text{ideal}}$ we obtain the optimization problem that should be solved at each sampling time to obtain the multi-stage NMPC feedback policy κ_{ms} :

$$\underset{\mathcal{U}(0), \dots, \mathcal{U}(N_p-1)}{\text{minimize}} \quad \sum_{k=0}^{N_p-1} \sum_{i=1}^{s^k} \ell(x_i(k), u_i(k)) + \sum_{i=1}^{s^{N_p}} V_f(x_i(N_p)), \quad (11a)$$

$$\mathbb{P}_{\text{ms}} : \quad \text{subject to} \quad \tilde{\mathcal{X}}(k+1) = \bigcup_{i=1}^{s^k} \bigcup_{j=1}^s f(x_i(k), u_i(k), d_j), \quad \text{for } k = 0, \dots, N_p - 1, \quad (11b)$$

$$g_l(\tilde{\mathcal{X}}(k), \mu(\tilde{\mathcal{X}}(k)), \tilde{D}) \leq 0, \quad l = 1, \dots, n_g, \quad \text{for } k = 0, \dots, N_p - 1, \quad (11c)$$

$$\tilde{\mathcal{X}}(N_p) \subseteq \mathcal{X}_f, \quad (11d)$$

$$\tilde{\mathcal{X}}(0) = \{\hat{x}(0)\}, \quad (11e)$$

where the constraints (11c) denote that $g_l(x, \mu(x), d) \leq 0$ should be satisfied for all $x \in \tilde{\mathcal{X}}(k)$ and for all $d \in \tilde{D}$, and $\mathcal{U}(k)$ denotes the set of control inputs in the tree at stage k .

To avoid the exponential growth of the tree with the prediction horizon, a usual additional simplifying assumption is to consider that the tree branches only up to a given stage (usually called robust horizon). While this simplification introduces further errors in the approximation of the reachable sets at each stage, it achieves good results in practice [10]. The current estimation error as well as the presence of future estimation errors should be also included in the problem formulation to achieve stability and recursive feasibility guarantees. This can be done in a multi-stage framework as shown in [45], but additional uncertainties should be included in the scenario tree. To mitigate the exponential growth of the scenario tree with the number of considered uncertainties, we do not consider the estimation error directly in the formulation of the tree. Following ideas from tube-based MPC, these additional errors will be taken into account by means of constraint tightening as explained in Section 4.

3 | DEEP LEARNING-BASED APPROXIMATE ROBUST NMPC

Despite recent advances in algorithms and hardware, solving the simplified output-feedback robust NMPC problem defined in (11) in real time can be challenging. To avoid the need for the real-time solution of non-convex optimization problems, this work considers the data-based approximation of the implicit feedback law defined by (11) following the same ideas as explicit model predictive control. Approximating an NMPC controller with a neural network was already proposed by [20] back in 1995, where the use of shallow networks (with only one hidden layer) was proposed. This suggestion is based on the universal approximation theory that shows that a neural network with only one layer can approximate any function with any desired accuracy under mild conditions [46].

Deep neural networks (DNNs) are chosen here as function approximators, motivated by recent theoretical results that support the increased representation power of neural networks with several hidden layers as opposed to classical shallow networks [23]. For the approximation of MPC laws via deep neural networks good results were obtained in [22, 39, 38, 21] among other recent works. In the case of linear time-invariant systems, it was shown in [21] that a deep neural network with a given size can exactly represent the explicit MPC law. The robust NMPC problem (11) is a parametric optimization problem that depends on the current (estimated) state and on the uncertainty values used to define the scenario tree. To perform a deep learning-based approximation, a finite amount of N_s samples x_i of the state space are chosen and then N_s different optimization problems are solved to obtain the corresponding optimal inputs $u_i^*(x_i)$.

A standard deep feed-forward neural network with fully connected layers is defined as a sequence of layers which determines a function $\mathcal{N} : \mathbb{R}^{n_x} \rightarrow \mathbb{R}^{n_u}$ of the form

$$\mathcal{N}(x; \theta) = \begin{cases} \alpha_{L+1} \circ \beta_L \circ \alpha_L \circ \dots \circ \beta_1 \circ \alpha_1(x) & \text{for } L \geq 2, \\ \alpha_{L+1} \circ \beta_1 \circ \alpha_1(x), & \text{for } L = 1, \end{cases} \quad (12)$$

where the input of the network is $x \in \mathbb{R}^{n_x}$ and the output of the network is $u \in \mathbb{R}^{n_u}$. The dimensions of the network are defined by the number of hidden layers L and the number of neurons H , also denoted as the width of the layer, per hidden layer, when equal width for all hidden layers is assumed. In contrast to *shallow* neural networks with $L = 1$ hidden layers, *deep* neural networks have $L \geq 2$ hidden layers. Each hidden layer connects a preceding affine function:

$$\alpha_l(\xi_{l-1}) = W_l \xi_{l-1} + b_l, \quad (13)$$

where $\xi_{l-1} \in \mathbb{R}^H$ is the output of the previous layer and $\xi_0 = x$, with a nonlinear activation function β_l . Common choices for the activation function are rectifier linear units (*ReLU*) and the sigmoid function hyperbolic tangent (*tanh*):

$$\beta_l(\alpha_l) = \frac{e^{\alpha_l} - e^{-\alpha_l}}{e^{\alpha_l} + e^{-\alpha_l}}, \quad (14)$$

which will be used throughout this work. The parameters of all layers are summarized in $\lambda = \{\lambda_1, \dots, \lambda_{L+1}\}$ with

$$\lambda_l = \{W_l, b_l\} \quad \forall l = 1, \dots, L+1, \quad (15)$$

where W_l are the weights and b_l are the biases describing the corresponding affine functions. The best data-based approximation of the exact multi-stage NMPC (11) with a neural network for a given training data set $\mathcal{T} = \{(x^{(1)}, u^*(x^{(1)})), \dots, (x^{(N_s)}, u^*(x^{(N_s)}))\}$ with N_s elements and fixed dimensions L and H is achieved for:

$$\lambda^* = \arg \min_{\lambda} \frac{1}{N_s} \sum_{i=1}^{N_s} (u^*(x^{(i)}) - \mathcal{N}(x^{(i)}; \lambda))^2. \quad (16)$$

The resulting deep learning-based controller is denoted as $\kappa_{\text{dnn}}(x) = \mathcal{N}(x; \lambda^*)$.

3.1 | Constraint tightening

We propose to use a robust NMPC scheme to take explicitly into account the most important uncertainties that affect the system. Still, it is virtually impossible to account for all possible uncertainties. Our goal is to determine a candidate controller by generating input-output data pairs via the solution of the multi-stage NMPC problem (11) and approximating its solution via a deep neural network solving (16). This means that the closed-loop will be controlled using the feedback law κ_{dnn} which can be different than the ideal, robust NMPC feedback law κ_{ideal} . In particular, we have three sources of errors:

$$\|\kappa_{\text{ideal}}(x(k)) - \kappa_{\text{dnn}}(\hat{x}(k))\| \leq \epsilon_{\text{est}} + \epsilon_{\text{ms}} + \epsilon_{\text{approx}}, \quad (17)$$

where ϵ_{est} is the error obtained because the estimation and measurement error are ignored in the multi-stage formulation (11), which is used to learn κ_{dnn} , to simplify its efficient implementation. The error due to the approximation of the reachable set by a set of discrete scenarios is denoted as ϵ_{ms} and finally the error due to the approximation of the solution of the optimization problem via a neural network is denoted as ϵ_{approx} . Finding upper-bounds for each one of the errors to apply traditional robust NMPC schemes is not possible for the general nonlinear case.

To counteract the possible errors ϵ_{est} , ϵ_{ms} , and ϵ_{approx} , and following ideas from tube-based MPC, an additional backoff η is used to tighten the original constraints of the robust NMPC problem that is solved to generate input-output data for training:

$$\underset{U_0, \dots, U_{N_p-1}}{\text{minimize}} \quad \sum_{k=0}^{N_p-1} \sum_{i=1}^{s^k} \ell(x_i(k), u_i(k)) + \sum_{i=1}^{s^{N_p}} V_f(x_i(N_p)), \quad (18a)$$

$$\mathbb{P}_{\text{ms}, \eta} : \quad \text{subject to} \quad \tilde{\mathcal{X}}(k+1) = \bigcup_{i=1}^{s^k} \bigcup_{j=1}^s f(x_i(k), u_i(k), d_j), \quad \text{for } k = 0, \dots, N_p - 1, \quad (18b)$$

$$g_l(\tilde{\mathcal{X}}(k), \mu(\tilde{\mathcal{X}}(k)), \tilde{D}) \leq -\eta, \quad l = 1, \dots, n_g, \quad \text{for } k = 0, \dots, N_p - 1, \quad (18c)$$

$$\tilde{\mathcal{X}}(0) = \{\hat{x}(0)\}. \quad (18d)$$

Solving (18) online would lead to the feedback controller $\kappa_{\text{ms}}(\hat{x}, \eta)$. We are however interested in the proposed approximate robust NMPC $\kappa_{\text{dnn}}(\hat{x}, \eta)$ that is obtained by training a deep neural network based on input-output data generated by solving (18) for many different initial conditions. Introducing a backoff η does not guarantee in general that the closed-loop satisfies the constraints. For this reason, closed-loop constraint satisfaction is also not ensured a priori with a terminal set. We propose, in the following sections, a probabilistic design scheme oriented to select the backoff parameter η . The presented methodology yields probabilistic guarantees for general performance indicators of the closed-loop uncertain system.

4 | CLOSED-LOOP PERFORMANCE INDICATORS

The goal of a robust output-feedback NMPC controller is that the closed-loop trajectory of the uncertain nonlinear system defined by

$$x(k+1) = f(x(k), \kappa(\hat{x}(k)), d(k)), \quad (19)$$

obtains a desired performance level, e.g. does not violate the predefined constraints, despite the presence of uncertainty, for any initial state $x(0)$ in the set \mathcal{X}_0 of feasible initial conditions, for any admissible initial estimation error $x(0) - \hat{x}(0)$ and for any sequence of uncertainty realizations $\{d(0), d(1), \dots, d(\infty)\}$.

Traditionally, robust NMPC schemes ensure that the closed-loop trajectory does not violate the constraints by solving the optimization problem (6) in a receding horizon fashion. The terminal set is chosen as a robust control invariant set that satisfies the constraints to prove recursive feasibility. The terminal and state cost satisfy certain conditions so that it can be proven that the optimal value of the cost function is a Lyapunov function and thus stability of the closed-loop can be guaranteed [41].

Solving problem (6) is in the general output-feedback nonlinear case intractable, and only approximations, like the one presented in (18), are possible. For this reason, we refrain from the idea of obtaining asymptotic performance guarantees. Instead, we focus on the use of finite-time closed-loop performance indicators that can be obtained by simulating the closed-loop system. The underlying assumption is that models which can be run a large number of times are available so that statistical guarantees can be obtained. A closed-loop performance indicator is defined as follows.

Definition 1 (Closed-loop finite-time performance indicator). Let $w = \{x(0), \hat{x}(0), d(0), \dots, d(N_{\text{sim}} - 1)\}$ denote the variables that define the closed loop trajectories $z(w; N_{\text{sim}}, \kappa) = \{x(0), \hat{x}(0), \kappa(\hat{x}(0)), d(0), x(1), \kappa(\hat{x}(1)), d(1), \dots, x(N_{\text{sim}})\}$ given an initial condition $x(0)$, an initial estimate $\hat{x}(0)$, a sequence of uncertainty realizations $d(0), \dots, d(N_{\text{sim}} - 1)$, a controller κ and a finite number of simulation steps N_{sim} . A closed-loop finite-time performance indicator is a measurable function $\phi(w; N_{\text{sim}}, \kappa) : \mathcal{W} = \mathbb{R}^{n_x} \times \mathbb{R}^{n_x} \times \mathbb{R}^{n_d} \times \dots \times \mathbb{R}^{n_d} \rightarrow \mathbb{R}$ that takes as input all variables of the closed-loop trajectories until time N_{sim} and gives a scalar as a measure of closed-loop performance:

$$\phi(w; N_{\text{sim}}, \kappa) = \phi(x(0), \hat{x}(0), \kappa(\hat{x}(0)), d(0), x(1), \kappa(\hat{x}(1)), d(1), \dots, x(N_{\text{sim}})). \quad (20)$$

Assumption 1. There exists a simulator that is able to compute closed-loop trajectories defined by (19). In addition, there exists a known operator Φ_k that provides the state estimation $\hat{x}(k+1)$ from $\hat{x}(k)$, $y(k)$ and $u(k)$. That is,

$$\hat{x}(k+1) = \Phi_k(\hat{x}(k), y(k), u(k)). \quad (21)$$

Assumption 1 implies that given N_{sim} and the controller κ , the closed-loop trajectories are completely determined by w . Probabilistic validation normally relies on a binary performance indicator that determines if the closed-loop is admissible or not. That is,

$$\phi(w; N_{\text{sim}}, \kappa) = \begin{cases} 0 & \text{if the closed-loop trajectory is admissible for } w, \\ 1 & \text{otherwise.} \end{cases}$$

For this particular setting, one can resort to well-known results to obtain probabilistic guarantees about the probability $\Pr_{\mathcal{W}}(\phi(w, N_{\text{sim}}, \kappa))$. For a review on these results, see [35]. See also [38], where Hoeffding's inequality [47] is used to derive probabilistic guarantees in the context of learning an approximate model predictive controller.

In this paper we address a more general setting in which we do not circumscribe the performance indicator to the class of binary functions. For example, we consider the closed-loop finite-time performance indicator given by the largest value of any component of g_l along the closed-loop simulation:

$$\phi(w; N_{\text{sim}}, \kappa) = \max_{\substack{k=0, \dots, N_{\text{sim}}-1 \\ l=1, \dots, n_g}} g_l(x(k), \kappa(\hat{x}(k)), d(k)). \quad (22)$$

Another possibility is to consider the average constraint violation as a performance indicator. That is,

$$\phi(w; N_{\text{sim}}, \kappa) = \frac{1}{N_{\text{sim}} n_g} \sum_{k=0}^{N_{\text{sim}}-1} \sum_{l=1}^{n_g} \max\{0, g_l(x(k), \kappa(\hat{x}(k)), d(k))\}. \quad (23)$$

Moreover, in many applications it is relevant to consider indicators related to the closed-loop cost, such as an average cost:

$$\phi(w; N_{\text{sim}}, \kappa) = \frac{1}{N_{\text{sim}}} \sum_{k=0}^{N_{\text{sim}}-1} \ell(x(k), \kappa(\hat{x}(k))), \quad (24)$$

or any other combination. In the following section we address how to obtain probabilistic guarantees on the random variable $\phi(w; N_{\text{sim}}, \kappa)$.

5 | PROBABILISTIC VALIDATION

Determining if a given controller provides admissible closed-loop trajectories, under the presence of nonlinearity and uncertainty, is in general an intractable problem [48]. In order to circumvent this issue, one can resort to probabilistic validation [25], [35], which provides probabilistic guarantees regarding the satisfaction of a given set of control specifications. In this section we present a novel result that allows us to address the probabilistic validation of the control scheme proposed in this paper.

We notice that the proposed controller is defined by means of some hyper-parameters: backoff η , number L of hidden layers in the network \mathcal{N} , etc. Therefore, we can consider a finite family of controllers

$$\kappa_i(\hat{x}), \quad i = 1, \dots, M,$$

corresponding to different choices of the hyper-parameters. The objective of this section is to provide a probabilistic validation scheme that allows us to choose, from the M possible controllers, the one with the best probabilistic certification for any given closed-loop finite-time performance indicator $\phi_i(w; N_{\text{sim}}, \kappa_i)$. For simplicity in the notation, we denote the closed-loop finite-time performance indicator obtained with the controller κ_i with N_{sim} simulation steps as $\phi_i(w)$.

Assumption 2. The stochastic variables w that define the closed-loop trajectories follow a certain probability distribution from which it is possible to obtain independent identically distributed (i.i.d.) samples.

Definition 2 (Probabilistic performance indicator level). We say that $\gamma \in \mathbb{R}$ is a probabilistic performance indicator level with violation probability $\epsilon \in (0, 1)$ for the measurable function $\phi : \mathcal{W} \rightarrow \mathbb{R}$ if

$$\Pr_{\mathcal{W}}\{\phi(w) > \gamma\} \leq \epsilon.$$

To obtain probabilistic performance indicator levels for the considered controllers κ_i , $i = 1, \dots, M$, we generate N i.i.d. scenarios

$$w^{(j)} = \{x^{(j)}(0), \hat{x}^{(j)}(0), d^{(j)}(0), \dots, d^{(j)}(N_{\text{sim}})\}, \quad j = 1, \dots, N.$$

For a given controller κ_i , with $1 \leq i \leq M$, and the uncertain realizations $w^{(j)}$, $j = 1, \dots, N$, one could simulate the closed-loop dynamics and obtain the performance indicator corresponding to each uncertain realization. That is, one could obtain

$$\mathbf{v}_i = [\phi_i(w^{(1)}), \phi_i(w^{(2)}), \dots, \phi_i(w^{(N)})]^\top \in \mathbb{R}^N.$$

It is clear that the largest value of the components of \mathbf{v}_i could serve as an empirical performance level for the controller κ_i provided that N is large enough [34]. Another possibility is to discard the $r - 1$ largest components of \mathbf{v}_i and consider the largest of the remaining components as a (less conservative) empirical performance indicator level (r equal to one corresponds to not discarding any component) [35]. In the following section we show how to choose N such that the obtained empirical performance indicator level are, with high confidence $1 - \delta$, probabilistic performance indicator levels with probability of violation ϵ .

5.1 | Probabilistic performance indicator levels: sample complexity

We first present a generalization of the notion of the maximum of a collection of scalars. This generalization is borrowed from the field of order statistics [49], [50], and will allow us to reduce the conservativeness that follows from the use of the standard notion of max function. See also Section 3 of [51].

Definition 3 (Generalized max function). Given the vector

$$\mathbf{v} = [v^{(1)}, v^{(2)}, \dots, v^{(N)}]^\top \in \mathbb{R}^N,$$

and the integer r with $1 \leq r \leq N$ we denote

$$\psi(\mathbf{v}, r) = v_+^{(r)},$$

where the vector $\mathbf{v}_+ = [v_+^{(1)}, v_+^{(2)}, \dots, v_+^{(N)}]^\top \in \mathbb{R}^N$ is obtained by rearranging the values of the components of \mathbf{v} in a non-increasing order. That is,

$$v_+^{(1)} \geq v_+^{(2)} \geq \dots \geq v_+^{(N-1)} \geq v_+^{(N)}.$$

Clearly, given $\mathbf{v} = [v^{(1)}, \dots, v^{(N)}]^\top \in \mathbb{R}^N$, we have

$$\psi(\mathbf{v}, 1) = \max_{1 \leq i \leq N} v^{(i)}, \quad \psi(\mathbf{v}, N) = \min_{1 \leq i \leq N} v^{(i)}.$$

Furthermore, $\psi(\mathbf{v}, 2)$ denotes the second largest value in \mathbf{v} , $\psi(\mathbf{v}, 3)$ the third largest one, etc. We notice that the notation $\psi(\mathbf{v}, r)$ does not need to make explicit N , the number of components of \mathbf{v} .

The next theorem provides a way to compute probabilistic performance levels for a family of M controllers. The theorem constitutes a generalization of a similar result, presented in [51] for the particular case $M = 1$. See also the seminal paper [34] for the particularization of the result to the case $r = 1$, $M = 1$.

Theorem 1. Given the controllers κ_i , $i = 1, \dots, M$, and the integer $r \geq 1$, suppose that N i.i.d. scenarios

$$w^{(j)} = \{x^{(j)}(0), \hat{x}^{(j)}(0), d^{(j)}(0), \dots, d^{(j)}(N_{\text{sim}})\}, \quad j = 1, \dots, N,$$

are generated. We denote with \mathbf{v}_i , $i = 1, \dots, M$, the vector of performance indicators corresponding to the controller κ_i . That is,

$$\mathbf{v}_i = [\phi_i(w^{(1)}), \phi_i(w^{(2)}), \dots, \phi_i(w^{(N)})]^\top \in \mathbb{R}^N, \quad i = 1, \dots, M.$$

Then, with probability no smaller than $1 - \delta$, we have

$$\Pr_{\mathcal{W}}\{\phi_i(w) > \psi(\mathbf{v}_i, r)\} \leq \epsilon, \quad i = 1, \dots, M,$$

provided that $1 \leq r \leq N$ and

$$\sum_{\ell=0}^{r-1} \binom{N}{\ell} \epsilon^\ell (1 - \epsilon)^{N-\ell} \leq \frac{\delta}{M}. \quad (25)$$

In addition, (25) is satisfied if:

$$N \geq \frac{1}{\epsilon} \left(r - 1 + \ln \frac{M}{\delta} + \sqrt{2(r-1) \ln \frac{M}{\delta}} \right). \quad (26)$$

Proof. Given the controller κ_i and $\gamma \in \mathbb{R}$, denote $E_i(\gamma)$ the probability of the event $\phi_i(w) > \gamma$. That is,

$$E_i(\gamma) \doteq \Pr_{\mathcal{W}}\{\phi_i(w) > \gamma\}.$$

Property 3 in [51] states that, with probability no smaller than

$$1 - \sum_{\ell=0}^{r-1} \binom{N}{\ell} \epsilon^\ell (1 - \epsilon)^{N-\ell},$$

we have

$$E_i(\psi(\mathbf{v}_i, r)) = \Pr_{\mathcal{W}}\{\phi_i(w) > \psi(\mathbf{v}_i, r)\} \leq \epsilon.$$

That is,

$$\Pr_{\mathcal{W}^N}\{E_i(\psi(\mathbf{v}_i, r)) > \epsilon\} \leq \sum_{\ell=0}^{r-1} \binom{N}{\ell} \epsilon^\ell (1 - \epsilon)^{N-\ell} \doteq B(N, \epsilon, r-1).$$

Consider now the probability δ_F that, after drawing N i.i.d. samples $w^{(i)}$, $i = 1, \dots, N$, one or more of the empirical performance indicator levels

$$\gamma_i = \psi(\mathbf{v}_i, r), \quad i = 1, \dots, M,$$

are not probabilistic performance indicator levels with violation probability ϵ . We have

$$\begin{aligned} \delta_F &= \Pr_{\mathcal{W}^N}\left\{\max_{i=1, \dots, M} E_i(\psi(\mathbf{v}_i, r)) > \epsilon\right\} \\ &\leq \sum_{i=1}^M \Pr_{\mathcal{W}^N}\{E_i(\psi(\mathbf{v}_i, r)) > \epsilon\} \\ &\leq M \sum_{\ell=0}^{r-1} \binom{N}{\ell} \epsilon^\ell (1 - \epsilon)^{N-\ell} \leq \delta. \end{aligned}$$

That is, δ_F is smaller or equal than δ provided that (25) holds. This proves the first claim of the property. The second one follows directly from Corollary 1 of [35], which provides an explicit number N of samples that guarantees that a binomial expression $B(N, \epsilon, r - 1)$ is smaller than a given constant. ■

Remark 1. Given a family of controllers $\kappa_i, i = 1, \dots, M$, one does not need to compute all the empirical performance indicator levels $\psi(\mathbf{v}_i, r), i = 1, \dots, M$. It is sufficient to find one that meets the desired performance indicator levels. For example, if the performance indicator $\phi_i(w)$ is defined as the average constraint violation along the trajectory (see (23)), then the controller κ_i provides an admissible closed-loop trajectory for w if and only if $\phi_i(w) = 0$. In this case, the empirical performance indicator $\psi(\mathbf{v}_i, r)$ corresponding to N i.i.d. scenarios is equal to 0 if no more than $r - 1$ trajectories are non admissible when applying the controller κ_i to the scenarios. If N is chosen according to (25) then Theorem 1 implies that with probability no smaller than $1 - \delta$, all the controllers $\kappa_i, i = 1, \dots, M$, providing $\psi(\mathbf{v}_i, r) = 0$ are such that

$$\Pr_{\mathcal{W}}(\phi_i(w) > 0) \leq \epsilon.$$

It is also important to remark that the cardinality M of the family of proposed controllers has little effect on the sample complexity N because it appears into a logarithm. See also Subsection 4.2 in [35] for other randomized approaches based on a design space of finite cardinality.

Remark 2. The probabilistic validation method presented here is completely independent on how the controllers κ_i are generated. Thus, the method is applicable not only to deep learning-based controllers, but to any possible control strategy. Nevertheless, the use of deep learning to approximate MPC controllers has been shown to have a promising performance compared to other approximation techniques [21], as we also illustrate in the remainder of the paper.

We now present a corollary from Theorem 1 that addresses the particular case in which the performance index $\phi_i(w)$ takes only binary values. The result presented in the corollary has been published in a slightly different form in [52] and has been used in different control design problems. See, for example, [36], [37].

Corollary 1. Given the controllers $\kappa_i, i = 1, \dots, M$, and the integer $r \geq 1$, suppose that N i.i.d. scenarios

$$w^{(j)} = \{x^{(j)}(0), \hat{x}^{(j)}(0), d^{(j)}(0), \dots, d^{(j)}(N_{\text{sim}})\}, j = 1, \dots, N,$$

are generated. Suppose also that the performance indicator $\phi_i : \mathcal{W} \rightarrow \{0, 1\}$ is defined as

$$\phi_i(w) = \begin{cases} 0 & \text{if the closed-loop trajectory corresponding to controller } \kappa_i \text{ and uncertainty realization } w \text{ is admissible,} \\ 1 & \text{otherwise.} \end{cases}$$

We denote with $\mathbf{v}_i, i = 1, \dots, M$, the vector of performance indicators corresponding to the controller κ_i . That is,

$$\mathbf{v}_i = [\phi_i(w^{(1)}), \phi_i(w^{(2)}), \dots, \phi_i(w^{(N)})]^\top \in \mathbb{R}^N, i = 1, \dots, M.$$

Denote S the set of indexes corresponding to the controllers for which no more than $r - 1$ trajectories are non admissible. That is, $S = \{i : 1 \leq i \leq M, \phi_i(\mathbf{v}_i, r) = 0\}$. Then, with probability no smaller than $1 - \delta$, we have

$$\Pr_{\mathcal{W}}\{\phi_i(w) = 1\} \leq \epsilon, \forall i \in S,$$

provided that $1 \leq r \leq N$ and

$$\sum_{\ell=0}^{r-1} \binom{N}{\ell} \epsilon^\ell (1 - \epsilon)^{N-\ell} \leq \frac{\delta}{M}. \quad (27)$$

In addition, (27) is satisfied if:

$$N \geq \frac{1}{\epsilon} \left(r - 1 + \ln \frac{M}{\delta} + \sqrt{2(r-1) \ln \frac{M}{\delta}} \right). \quad (28)$$

Proof. The proof follows directly from Theorem 1. From (27) and Theorem 1 we have that, with probability no smaller than $1 - \delta$,

$$\Pr_{\mathcal{W}}\{\phi_i(w) > \psi(\mathbf{v}_i, r)\} \leq \epsilon, i = 1, \dots, M.$$

This implies

$$\Pr_{\mathcal{W}}\{\phi_i(w) > \psi(\mathbf{v}_i, r)\} \leq \epsilon, \forall i \in S.$$

By definition, $\psi(\mathbf{v}_i, r) = 0$, for all $i \in S$. Thus,

$$\Pr_{\mathcal{W}}\{\phi_i(w) > 0\} \leq \epsilon, \forall i \in S.$$

Since $\phi_i(w) \in \{0, 1\}$ we conclude

$$\Pr_{\mathcal{W}}\{\phi_i(w) = 1\} \leq \epsilon, \forall i \in S.$$

The second claim follows from the second claim of Theorem 1. ■

Remark 3. We notice that Theorem 1 has some advantages when compared with Corollary 1:

- (i) With the same sample complexity, it is not limited to binary performance indicators.
- (ii) It is more informative, that is, it provides not only a probabilistic certification, but also the corresponding probabilistic performance indicator level.

6 | CASE STUDY

We investigate the optimal control of a kite which is used to tow a boat. The stable and safe operation of the kite is challenging due to the highly nonlinear system dynamics, uncertain parameters, strong influence from disturbances like wind speed and noisy measurements. Because short control intervals are necessary to steer the kite optimally, simpler models [53, 30] are preferred in the NMPC setup to reduce the computational load. We derive an approximate deep learning-based controller from a robust NMPC formulation, which enables a very fast and easy evaluation of the controller even on computationally limited hardware. The idea of learning a controller for a kite has already been exploited in [54], where polynomial basis functions were used to approximate the behaviour of a human pilot based on measurements. In the context of NMPC, we focus on the model presented in [55] which consists of the three ordinary differential equations of the three angles θ_{kite} , ϕ_{kite} and ψ_{kite} of the spherical coordinate system describing the position of the kite:

$$\dot{\theta}_{\text{kite}} = \frac{v_a}{L_T} (\cos \psi_{\text{kite}} - \frac{\tan \theta_{\text{kite}}}{E}), \quad (29a)$$

$$\dot{\phi}_{\text{kite}} = -\frac{v_a}{L_T \sin \theta_{\text{kite}}} \sin \psi_{\text{kite}}, \quad (29b)$$

$$\dot{\psi}_{\text{kite}} = \frac{v_a}{L_T} \tilde{u} + \dot{\phi}_{\text{kite}} \cos \theta_{\text{kite}}, \quad (29c)$$

where

$$v_a = v_0 E \cos \theta_{\text{kite}}, \quad (29d)$$

$$E = E_0 - \tilde{c} \tilde{u}^2. \quad (29e)$$

The angle between wind and tether (zenith angle) is described by θ_{kite} , the angle between the vertical and the plane is denoted by ϕ_{kite} and ψ_{kite} represents the orientation of the kite. The area of the kite is denoted as A , and L_T is the length of the tether. The effect of the wind is described by v_a . The glide ratio E is dependent on the uncertain base glide ratio E_0 and the magnitude of the steering deflection \tilde{u} [56]. The parameters of the kite model are shown in the upper part of Table 1.

The wind model was presented in [57] and is described by:

$$v_0 = v_m + \bar{v}_N + \sigma_v c_v p_v, \quad (30a)$$

where

$$\sigma_v = k_{\sigma_v} v_m, \quad (30b)$$

$$\bar{v}_N = -\sigma_v / (2v_m), \quad (30c)$$

$$\tau_F = L_v / v_m, \quad (30d)$$

$$K_F = \sqrt{1.49 \tau_F / T_v}, \quad (30e)$$

$$c_v = K_F / \tau_F, \quad (30f)$$

$$\dot{p}_v = -p_v / \tau_F + w_{\text{tb}}, \quad (30g)$$

when the wind shear is neglected. The term w_m gives the current average wind speed, w_{tb} is introduced as a white noise generator to model the short term turbulence and $p_v(0) = \text{normal}(0, 0.25)$ is the initial state of the turbulence, where $x_{\text{normal}} = \text{normal}(\mu_{\text{normal}}, \sigma_{\text{normal}})$ denotes that the variable x_{normal} follows a normal distribution with mean μ_{normal} and standard deviation σ_{normal} . In a similar manner, $x_{\text{unif}} = \text{unif}(a_{\text{unif}}, b_{\text{unif}})$ means that the variable x_{unif} follows a uniform distribution between a_{unif} and b_{unif} . An overview of the parameters for the wind model is given in the lower part of Table 1. For further details on modeling assumptions and the choice of parameters the reader is referred to [57].

For the simulation of the system, it is assumed that the uncertain parameters E_0 and w_m are constant over a given closed-loop simulation and that w_{tb} changes every $t_c = 0.15$ s. The values of the uncertain parameters are drawn from the probability distribution described in Table 1.

To build a multi-stage NMPC controller, we consider the combinations of the extreme values of the base glide ratio $E_0 \in [4, 6]$ and the wind speed $v_0 \in [6 \text{ m s}^{-1}, 10 \text{ m s}^{-1}]$ resulting in a total of four scenarios. The interval for the wind speed is obtained by summarizing the possible effects of the uncertain wind model parameters v_m , $p_v(0)$ and w_{tb} into the single uncertain variable v_0 .

We assume that we can measure the two angles θ_{kite} and ϕ_{kite} and the wind speed v_0 . An Extended Kalman Filter (EKF) is used to obtain an estimate of the augmented state $x_{\text{aug}} = [\theta_{\text{kite}}, \phi_{\text{kite}}, \psi_{\text{kite}}, E_0, v_0]^T$ in each control instance from the measurements:

$$y(x_{\text{aug}}) = [\theta_{\text{kite}} + w_{\theta_{\text{kite}}}, \phi_{\text{kite}} + w_{\phi_{\text{kite}}}, v_0 + w_{v_0}]^T, \quad (31)$$

with the zero-mean gaussian noises $w_{\theta_{\text{kite}}} = \text{normal}(0, 0.01)$, $w_{\phi_{\text{kite}}} = \text{normal}(0, 0.01)$ and $w_{v_0} = \text{normal}(0, 0.05)$. The augmented state is initialized for all simulations as $x_{\text{aug}}(0) = [\theta_{\text{kite}}(0) \cdot \delta_{\theta_{\text{kite}}}, \phi_{\text{kite}}(0) \cdot \delta_{\phi_{\text{kite}}}, \psi_{\text{kite}}(0) \cdot \delta_{\psi_{\text{kite}}}, E_0 \cdot \delta_{E_0}, v_0(0) \cdot \delta_{v_0}]^T$, where all noises $\delta_{(\cdot)}$ are drawn from $\text{normal}(1, 0.05)$. Neither the estimates of the uncertain parameters nor the measurement of the wind speed are used in the computations of the controller, because their possible values are considered in the robust NMPC approach. The initial covariance matrix is given by $P_{\text{EKF}} = \text{diag}([1 \times 10^{-2}, 1 \times 10^{-2}, 1 \times 10^{-2}, 1.0, 2 \times 10^{-1}])$, the estimate of the process noise by $Q_{\text{EKF}} = \text{diag}([1 \times 10^{-5}, 1 \times 10^{-5}, 1 \times 10^{-4}, 1 \times 10^{-5}, 3 \times 10^{-3}])$, the measurement noise matrix by $R_{\text{EKF}} = \text{diag}([1 \times 10^{-2}, 1 \times 10^{-2}, 5 \times 10^{-2}])$ and the observer has a sampling time of $t_{\text{EKF}} = 0.05$ s. The goal of the control is to maximize the thrust of the tether defined by:

$$T_F = \frac{1}{2} \rho v_0^2 A \cos^2 \theta_{\text{kite}} (E + 1) \sqrt{E^2 + 1} \cdot (\cos \theta_{\text{kite}} \cos \beta + \sin \theta_{\text{kite}} \sin \beta \sin \phi_{\text{kite}}), \quad (32)$$

while maintaining a smooth control performance and satisfying the constraints. The desired behaviour is enforced in the stage cost:

$$\ell(x, u) = -w_F T_F + w_u (\tilde{u} - \tilde{u}_{\text{prev}})^2, \quad (33)$$

where $w_F = 1e-4$ and $w_u = 0.5$ are weights and \tilde{u}_{prev} is the previous control input and sampling time of the controller $t_c = 0.15$ s with a prediction horizon of $N_p = 40$ steps. Throughout the operation of the kite it has to be ensured that the height of the kite:

$$h(x) = L_T \sin \theta_{\text{kite}} \cos \phi_{\text{kite}}, \quad (34)$$

never falls below $h_{\text{min}} = 100$ m. The height constraint is a critical constraint of the control task since the best performance is obtained when the kite is operated close to h_{min} . Because of the error ϵ_{ms} caused by the approximation of the reachable sets in the multi-stage NMPC formulation, the errors due to a deep learning-based approximation ϵ_{approx} as well as the errors related to estimation and measurement errors ϵ_{est} , constraint satisfaction can not be guaranteed. To cover the effect of the errors, the backoff parameter $\eta > 0$ m is introduced and the height constraint:

$$h(x) > h_{\text{min}} + \eta, \quad (35)$$

is formulated as a soft constraint to avoid numerical problems.

7 | RESULTS

7.1 | Learning an approximate output-feedback robust NMPC controller

The training process of a neural network is determined by the quality of the data and the chosen hyperparameters like activation function of the hidden layers and network size. In the following, we discuss how the training data can be generated in a way that reduces the number of samples that are needed to achieve a satisfactory approximation in comparison to a random sampling and we also show that deep neural networks achieve a better approximation of the data than shallow ones. For the training of the

TABLE 1 Overview of the model states and parameters.

	Symbol	Type	Values / Constraints	Units
kite model	θ_{kite}	State	$[0, \frac{\pi}{2}]$	rad
	ϕ_{kite}	State	$[-\frac{\pi}{2}, \frac{\pi}{2}]$	rad
	ψ_{kite}	State	$[0, 2\pi]$	rad
	\tilde{u}	Control input	$[-10, 10]$	N
	\tilde{c}	Known parameter	0.028	-
	β	Known parameter	0	rad
	ρ	Known parameter	1	kg m ⁻³
	h_{min}	Known parameter	100	m
wind model	E_0	Uncertain parameter	unif(4, 6)	-
	p_v	State	-	s
	k_{σ_v}	Known parameter	0.14	-
	L_v	Known parameter	100	m
	T_v	Known parameter	0.15	s
	v_m	Uncertain parameter	unif(7, 9)	m s ⁻¹
	w_{tb}	Uncertain parameter	normal(0, 0.25)	-

neural networks we used the toolbox Keras [58] with the backend TensorFlow [59] and Adam [60] as the optimization algorithm. All considered networks use hyperbolic tangent (*tanh*) as activation function in the hidden layers and a linear output layer.

Each data sample is a pair $(\kappa_{\text{ms}}(x^{(i)}), x^{(i)})$ corresponding to the numerical solution of the multi-stage problem (18) at state $x^{(i)}$. The data set $\mathcal{T}_{\text{feas}} = \{(\kappa_{\text{ms}}(x^{(i)}), x^{(i)}), \dots, (\kappa_{\text{ms}}(x^{(N_s)}), x^{(N_s)})\} = \{z^{(i)}, \dots, z^{(N_s)}\}$ is obtained by sampling $x^{(i)}$ uniformly from the feasible state space. The data set $\mathcal{T}_{\text{opt}} = \{z^{(i)}, \dots, z^{(N_{\text{traj}})}\}$ contains data from state-feedback closed-loop simulations of the exact controller (11) under the dynamics presented in (29), where the uncertain parameters of the model and the initial conditions are drawn according to the distributions given in Table 1 and first row of Table 3 respectively. Since the training data is generated based on simulations, the application of output-feedback via EKF is superfluous and not used for the data generation. Each trajectory consists of $N_{\text{sim}} = 400$ simulation steps which results in a total simulation time of $t_{\text{sim}} = N_{\text{sim}} \cdot t_c = 60$ s. $N_{\text{traj}} = 200$ closed loop runs were simulated leading to $N_s = N_{\text{traj}} \cdot N_{\text{sim}} = 80000$ data pairs.

Training a deep neural network with $L = 6$ layers and $H = 30$ neurons per layer with the data pairs \mathcal{T}_{opt} leads to a significantly smaller average mean squared error (MSE) when compared to the training using the training data $\mathcal{T}_{\text{feas}}$, as Figure 2a shows, because the sampled space of optimal trajectories is smaller in comparison to the feasible space. That \mathcal{T}_{opt} is not covering the whole feasible space is not critical since the approximate controller will operate in the space of optimal trajectories and it will be anyway probabilistically validated. This means that extracting training data from closed loop trajectories can reduce the necessary number of training data N_s and dimensions L and H of the neural network to obtain a desired approximation error of the deep learning-based controller.

The second major influence of the training process is structure and size of the chosen neural network. The complexity of a neural network can be defined either by the number of weights

$$N_{\text{weights}} = n_x \cdot (H + 1) + (L - 1) \cdot (H + 1) \cdot H + H \cdot (n_u + 1),$$

or the number of neurons

$$N_{\text{neurons}} = L \cdot H,$$

that form a given network. The number of weights defines the necessary memory that is needed to store a neural network while the number of neurons determines the amount of nonlinear functions present in the approximation. We designed two shallow networks ($L = 1$) which have equal complexity with respect to the number of weights N_{weights} or the number of neurons N_{neurons} when compared to a deep neural network $\mathcal{N}_{\text{deep}}$ with $H = 30$ neurons per layer and $L = 6$ hidden layers. The resulting networks $\mathcal{N}_{\text{shallow},1}$ with $N_{\text{neurons}} = 180$ neurons, $\mathcal{N}_{\text{shallow},2}$ with $N_{\text{weights}} = 960$ and the $\mathcal{N}_{\text{deep}}$ were trained on the data set D_{opt} . The deep neural network clearly outperforms both shallow networks with respect to the MSE, as can be seen in Figure 2b.

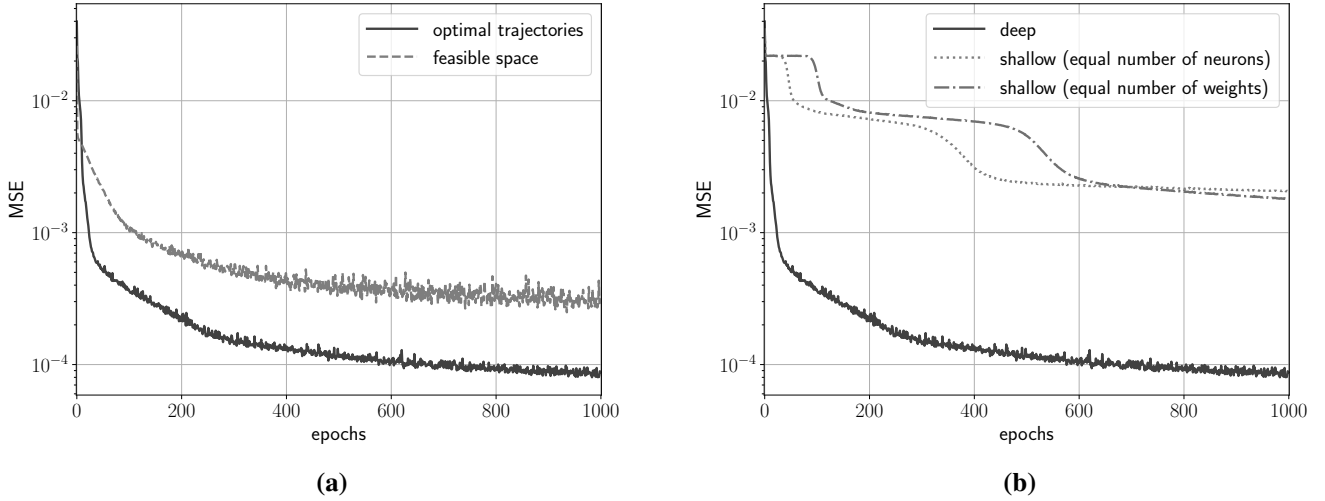


FIGURE 2 Mean squared error obtained when training a deep neural network using the space of optimal trajectories \mathcal{T}_{opt} or the full feasible space $\mathcal{T}_{\text{feas}}$ as training data (a). Comparison of the mean squared error for deep neural network and two shallow networks with comparable complexity (b). The training of all networks has been performed five times and averaged.

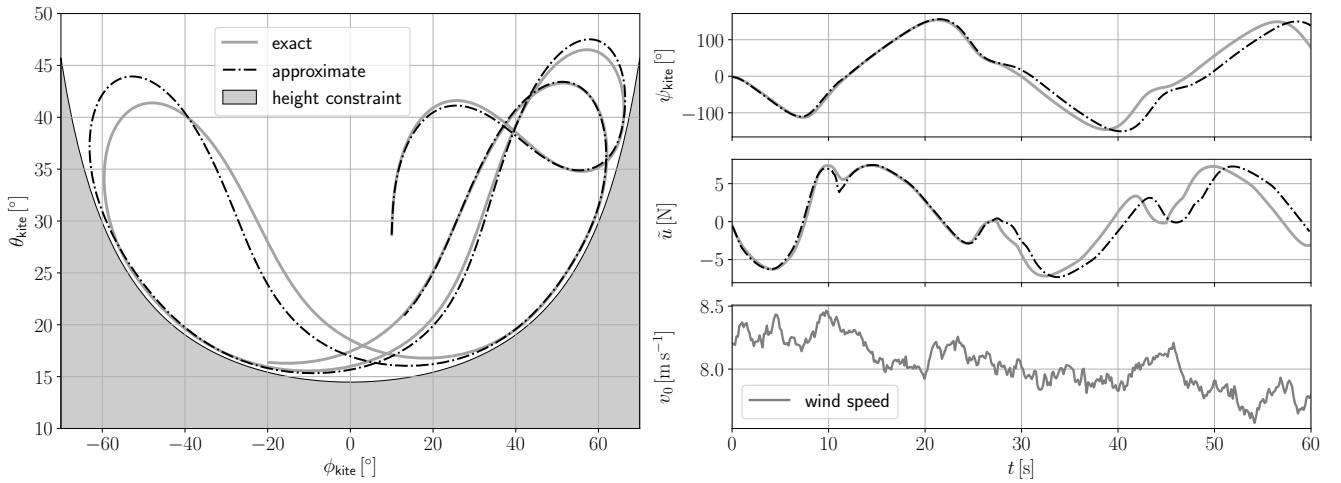


FIGURE 3 Comparison of the exact multi-stage NMPC and its deep learning-based approximation for one sample w and backoff $\eta = 4$ m. The left plot shows the state trajectory with the height constraint and the right plot shows the temporal evolution of the orientation ψ_{kite} , the control \tilde{u} and the wind speed v_0 .

The following subsections include exclusively results for deep neural networks which were trained on the space of optimal trajectories \mathcal{D}_{opt} due to the observed superior training performance. The design parameters for all networks are $L = 6$ hidden layers with each $H = 30$ neurons. A comparison of the performance of the exact multi-stage NMPC and the learning-based approximation, both with backoff $\eta = 4$ m, is shown in Figure 3. The exact multi-stage NMPC is obtained by solving (18) at each sampling time. Both controllers use the same EKF to estimate the states as described in Section 6. The deviation between the trajectories of the controllers is caused by the effect of the approximation error ϵ_{approx} which accumulates over time. However, the trajectory of the approximate controller satisfies the constraints and will be probabilistically validated in the next subsection.

7.2 | Verification of a deep learning-based embedded output-feedback robust NMPC

Because of the approximation errors, measurement and estimation errors as well as the errors derived from the multi-stage formulation, we refrain from a worst-case deterministic analysis and resort to the probabilistic verification scheme based on closed-loop trajectories presented in Section 5. We consider a family of $M = 4$ deep learning-based approximate controllers $\kappa_{\text{dnn},\eta}$ which were trained on data sets $\mathcal{T}_{\text{opt},\eta}$ with backoffs $\eta = \{0 \text{ m}, 2 \text{ m}, 4 \text{ m}, 6 \text{ m}\}$ with each 80000 data pairs. The resulting controllers were analyzed for N i.i.d. scenarios $w^{(j)}$, $j = 1, \dots, N$ corresponding to N closed-loop simulations under the dynamics presented in (29), where the uncertain parameters of the model and the initial conditions are drawn according to the distributions given in Table 1 and first row of Table 3 respectively. Since the height constraint (35) is the most critical constraint, we define the performance indicator:

$$\phi(w; N_{\text{sim}}, \kappa_{\text{dnn},\eta}) = \max_{j=0, \dots, N_{\text{sim}}} (h_{\min} - h(x(j, w))), \quad (36)$$

where $x(j, w)$ is the state trajectory at sampling time j caused by scenario w using controller $\kappa_{\text{dnn},\eta}$. The performance indicator (36) extracts the largest violation of the minimum height h_{\min} , if a violation occurs, or the closest approximation to h_{\min} throughout one scenario. Each scenario has a duration of 60 s equalling $N_{\text{sim}} = 400$. To consider a controller probabilistically safe, we require that the probabilistic performance indicator satisfies:

$$\Pr_{\mathcal{W}}(\phi(w; N_{\text{sim}}, \kappa_{\text{dnn},\eta}) > 0) \leq \epsilon, \quad (37)$$

with confidence $1 - \delta$ for a randomly sampled scenario w according to $\Pr_{\mathcal{W}}$. Following the notation of Theorem 1, the performance indicators corresponding to backoff parameters $\{0 \text{ m}, 2 \text{ m}, 4 \text{ m}, 6 \text{ m}\}$ are collected into vectors $\{\mathbf{v}_1, \mathbf{v}_2, \mathbf{v}_3, \mathbf{v}_4\}$ respectively. We consider a value of the discarding parameter $r = 4$. That is, a controller is probabilistically validated if no more than 3 simulations violate the height constraint. For these specifications ($\epsilon = 0.02$, $\delta = 1 \times 10^{-6}$, and $r = 4$), $N = 1388$ samples are required (see (28)). The family of controllers was evaluated for 1388 i.i.d. scenarios $w^{(j)}$ and the results are summarized in Table 2. If no backoff is considered ($\eta = 0 \text{ m}$), violations of the height constraint occur in more than half of the scenarios which was predictable because of the accumulation of errors ϵ_{ms} , ϵ_{approx} and ϵ_{est} . By considering $\eta = 2 \text{ m}$, the amount of violations can be significantly reduced to 8 scenarios, which shows the importance of the backoff parameter. However, the performance of $\kappa_{\text{dnn},2}$ is not considered probabilistic safe because after discarding the allowed number of worst-case simulation runs, we get $\psi(\mathbf{v}_2, 4) = 0.273 \text{ m} > 0 \text{ m}$. With larger backoffs $\eta = 4 \text{ m}$ and $\eta = 6 \text{ m}$, we obtain two probabilistically safe controllers with performance indicator levels $\psi(\mathbf{v}_3, 4) = -0.316 \text{ m}$ and $\psi(\mathbf{v}_4, 4) = -1.818 \text{ m}$, respectively. The preferred deep learning-based controller is $\kappa_{\text{dnn},4}$ due to the higher average tether thrust T_F provided. By introducing a performance indicator level for the average thrust per simulation run:

$$\phi_{T_F}(w; N_{\text{sim}}, \kappa) = \frac{1}{N_{\text{sim}}} \sum_{k=0}^{N_{\text{sim}}-1} -T_F(k), \quad (38)$$

it is possible to obtain probabilistic statements about the performance in the same fashion as for violation of the height constraint. Using the parameters $\delta = 1 \times 10^{-6}$, $\epsilon = 0.02$, $M = 4$ and $r = 4$ we obtain, for the controller $\kappa_{\text{dnn},4}$, that with confidence $1 - \delta$, the probability that the average thrust for a simulation run of 60 s duration is lower than 111.346 kN is not larger than $\epsilon = 0.02$. A smaller number of samples is required if the discarding parameter r is set equal to 1. However, this leads to more conservative results because violations of the height constraint occur throughout the closed loop simulations used for verification. This is even worse when the performance index is a binary function determining if the trajectories are admissible or not. In this case, the obtained results are often not informative because in a binary setting with $r = 1$, a single violated trajectory out of N determines that the controller does not meet the probabilistic constraints. Larger values for r , along with the consideration of non-binary violation performance indexes, provide more informative results. One more advantage of the proposed probabilistic method is that a family of controllers can be evaluated in parallel in the closed loop for the same set of sampled scenarios. This can reduce the verification effort significantly, if drawing samples w from \mathcal{W} is costly or the closed-loop experiments have a long duration.

7.3 | Robustness of the probabilistic validation scheme

All obtained probabilistic guarantees are only valid if the assumptions about the probability density functions (PDFs) of \mathcal{W} from which the scenarios w are drawn are correct. For the verification, the N closed-loop simulations were generated using the dynamics presented in (29) and the different $\kappa_{\text{dnn},\eta}$ controllers. The uncertain parameters of the model and the initial conditions were drawn according to the distributions given in Table 1 and first row of Table 3 respectively.

TABLE 2 Comparison of the members of a deep learning-based family of controllers defined by $M = 4$ different choices of the backoff parameter $\eta = \{0 \text{ m}, 2 \text{ m}, 4 \text{ m}, 6 \text{ m}\}$. The parameters for the probabilistic safety certificate were chosen to $\epsilon = 0.02$ and $\delta = 1 \times 10^{-6}$. The necessary number of samples for 3 discarded worst-case runs ($r = 4$) is $N = 1388$ and computed via (28).

controller	$\kappa_{\text{dnn},0}$	$\kappa_{\text{dnn},2}$	$\kappa_{\text{dnn},4}$	$\kappa_{\text{dnn},6}$
feasible trajectories	660/1388	1380/1388	1385/1388	1387/1388
$\psi(\mathbf{v}, 4)$ [m]	1.682	0.273	-0.316	-1.818
T_F (avg.) [kN]	227.516	225.997	224.185	222.179
probabilistically safe	No	No	Yes	Yes

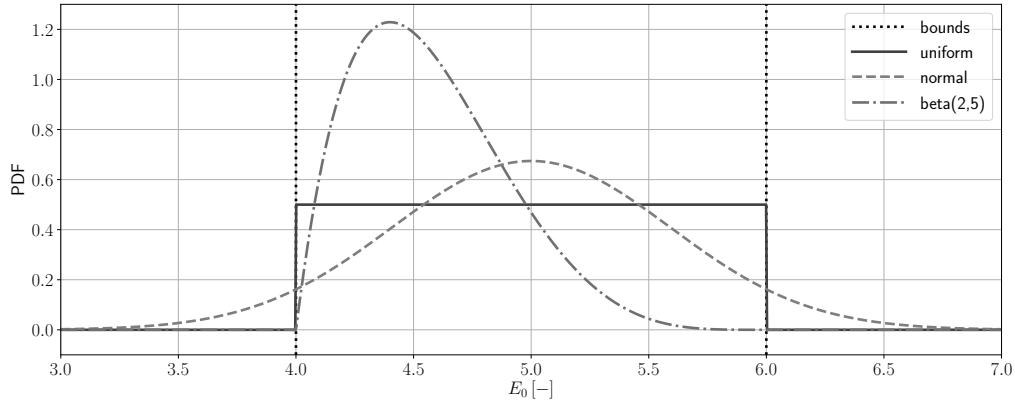


FIGURE 4 Three different considerations of the uncertain parameter base glide ratio E_0 and the considered bounds in the NMPC formulation. Only the normal distribution exceeds the considered bounds.

To test the robustness of the probabilistic statements w.r.t. to wrong assumptions about the PDFs, the performance of the approximate controllers $\kappa_{\text{dnn},\eta}$ is evaluated using not the distribution of the first row of Table 3, but the second (normal distribution) and the third one (beta distribution). The first parameter in the description of the beta distribution is the scaling and the second parameter is the offset, e.g.

$$\theta_0 = 2.0 \cdot \text{beta}(2, 5) + 28.0.$$

The possible extreme values of samples from the space of beta distributions $\mathcal{W}_{\text{beta}}$ are identical with those when sampling from the space of uniform distributions \mathcal{W} , see Figure 4. In case of sampling from $\mathcal{W}_{\text{normal}}$, which has infinite support, the occurrence of values in w which exceed the bounds of the scenarios considered in the robust MPC formulation and the verification scenarios is likely, which highlights the importance of including the discarding parameter r . The three different considered PDFs including the bounds applied in the NMPC formulation are shown in Figure 4 for the example base glide ratio E_0 .

The results corresponding to drawing 1388 scenarios from each of the distributions $\mathcal{W}_{\text{normal}}$ and $\mathcal{W}_{\text{beta}}$, and evaluating the approximate controller $\kappa_{\text{dnn},4}$ are given in Table 3. For both alternative scenario spaces one simulation run violates the height constraint. This means that the probabilistic requirements for the safety certificate ($\epsilon = 0.02$, $\delta = 1 \times 10^{-6}$, $M = 4$, $r = 4$) hold for both choices of distributions. This shows that neither the training of the network nor the verification approach fails catastrophically when the statistical assumptions are not exactly fulfilled.

7.4 | Embedded implementation

One of the major advantages of learning the complex optimal control law via deep neural networks is the reduction of computational load and the fast evaluation. The computation of the control input is reduced from solving an optimization problem to one matrix-vector multiplication per layer and the evaluation of the \tanh -function. This enables the implementation of a probabilistically validated, approximate robust nonlinear model predictive control on limited hardware such as microcontrollers or field

TABLE 3 Overview of the the parameter sampling via uniform distribution, normal distribution and beta(2,5) distribution and results of evaluating the approximate controller κ_{dnn} with $\eta = 4$ m for 1388 randomly drawn scenarios w . The measurement noise $w_{\text{meas}} = [w_{\theta_{\text{kite}}}, w_{\phi_{\text{kite}}}, w_{\psi_{\text{kite}}}]^T$, the initial state of the turbulence $p_v(0) = \text{normal}(0, 0.25)$, the white noise modelling the short term turbulences $w_{\text{tb}} = \text{normal}(0, 0.25)$ and the initialization of the estimation vector $x_{\text{aug}}(0)$ is for all scenario spaces identical.

distribution	$\theta_{\text{kite}}(0)$ [°]	$\phi_{\text{kite}}(0)$ [°]	$\psi_{\text{kite}}(0)$ [°]	E_0 [-]	v_m [m s ⁻¹]	feasible traj.	$\psi(v, 4)$ [m]
Uniform	(28.0,30.0)	(-10.0,10.0)	(-2.0,2.0)	(4.0,6.0)	(7.0,9.0)	1385/1388	-0.316
Normal	(29.0,0.35)	(0.0,3.5)	(0.0,0.7)	(5.0,0.35)	(8.0,0.35)	1387/1388	-0.739
Beta	(2.0,28.0)	(20.0,-10.0)	(4.0,-2.0)	(2.0,4.0)	(2.0,7.0)	1387/1388	-0.556

programmable gate arrays (FPGAs). We deployed the approximate controller on a low-cost microcontroller (ARM Cortex-M3 32-bit) running with a frequency of 89 MHz with 96 kB RAM. The memory footprint of both the EKF and the neural network that describes the approximate robust NMPC is only 67.0 kB of the 512 kB flash memory. The implementation was tested in a hardware-in-the-loop environment. The average time needed to evaluate the neural network was 32.1 ms (max. evaluation time: 33.0 ms) and the average evaluation time for one EKF step was 28.3 ms (max. evaluation time: 30.0 ms), which shows that the proposed controller is real-time capable.

8 | CONCLUSIONS AND FUTURE WORK

The computation complexity related to output-feedback robust NMPC controllers is prohibitive in most cases. Instead of relying on strong assumptions on error bounds and invariant sets that cannot be verified in practice, we propose to compute an approximate robust NMPC controller based on a tree of discrete scenarios that can be verified a posteriori. To enable the implementation of such controllers in real-time even on limited embedded hardware, we used deep learning to approximate the proposed robust NMPC controller.

To deal with errors related to estimation, computation of approximate reachable sets based on scenarios as well as approximation of the resulting optimization problem with a neural network, we tighten the original constraints of the problem using a backoff parameter. One of the main contributions of this paper is a probabilistic validation methodology that can be used with general performance indicators. Probabilistic guarantees about the performance of the closed-loop can be given, which are less restrictive than previous approaches because of the incorporation of a discarding parameter and the consideration of non-binary performance indicators. Moreover, the required sample complexity does not depend on the dimension of the problem. The promising results for the embedded output-feedback robust NMPC of a towing kite show the potential of the proposed approach. Future work includes the definition of robust margins based on probabilistic validation techniques as well as the learning of controllers that are parameterized, for example, with a backoff parameter.

ACKNOWLEDGMENTS

Teodoro Alamo acknowledges MEyC Spain (contract DPI2016-76493-C3-1-R).

Financial disclosure

None reported.

Conflict of interest

The authors declare no potential conflict of interests.

References

- [1] P. J. Campo and M. Morari, “Robust model predictive control,” in *Proc. of the American Control Conference*, 1987, pp. 1021–1026.
- [2] J. H. Lee and Z. H. Yu, “Worst-case formulations of model predictive control for systems with bounded parameters,” *Automatica*, vol. 33, no. 5, pp. 763–781, 1997.
- [3] D. Q. Mayne, M. M. Seron, and S. V. Rakovic, “Robust model predictive control of constrained linear systems with bounded disturbances,” *Automatica*, vol. 41, pp. 219 – 224, 2005.
- [4] S. Rakovic, B. Kouvaritakis, M. Cannon, C. Panos, and R. Findeisen, “Fully parameterized tube MPC,” in *Proc. of the 18th IFAC World Congress Milano*, 2011, pp. 197–202.
- [5] J. Fleming, B. Kouvaritakis, and M. Cannon, “Robust tube MPC for linear systems with multiplicative uncertainty,” *IEEE Transactions on Automatic Control*, vol. 60, no. 4, pp. 1087–1092, 2015.
- [6] P. Scokaert and D. Mayne, “Min-max feedback model predictive control for constrained linear systems,” *IEEE Transactions on Automatic Control*, vol. 43, no. 8, pp. 1136–1142, 1998.
- [7] D. Muñoz de la Peña, A. Bemporad, and T. Alamo, “Stochastic programming applied to model predictive control,” in *Proc. of the 44th IEEE Conference on Decision and Control*, 2005, pp. 1361–1366.
- [8] D. Bernardini and A. Bemporad, “Scenario-based model predictive control of stochastic constrained linear systems,” in *Proc. of the 48th IEEE Conference on Decision and Control*, 2009, pp. 6333–6338.
- [9] S. Lucia, T. Finkler, and S. Engell, “Multi-stage nonlinear model predictive control applied to a semi-batch polymerization reactor under uncertainty,” *Journal of Process Control*, vol. 23, pp. 1306–1319, 2013.
- [10] S. Lucia, J. Andersson, H. Brandt, M. Diehl, and S. Engell, “Handling uncertainty in economic nonlinear model predictive control: a comparative case-study,” *Journal of Process Control*, vol. 24, pp. 1247–1259, 2014.
- [11] P. Goulart, E. C. Kerrigan, and J. M. Maciejowski, “Optimization over state feedback policies for robust control with constraints,” *Automatica*, vol. 42, pp. 523–533, 2006.
- [12] S. Lucia, *Robust Multi-stage Nonlinear Model Predictive Control*. Shaker, 2014.
- [13] B. Houska, H. Ferreau, and M. Diehl, “An auto-generated real-time iteration algorithm for nonlinear MPC in the microsecond range,” *Automatica*, vol. 47, pp. 2279–2285, 2011.
- [14] J. Mattingley and S. Boyd, “Cvxgen: A code generator for embedded convex optimization,” *Optimization and Engineering*, vol. 13, no. 1, pp. 1–27, 2012.
- [15] P. Zometa, M. Kögel, and R. Findeisen, “muAO-MPC: A free code generation tool for embedded real-time linear model predictive control,” in *Proc. of the American Control Conference*, 2013, pp. 5320–5325.
- [16] S. Lucia, D. Navarro, O. Lucia, P. Zometa, and R. Findeisen, “Optimized FPGA implementation of model predictive control using high level synthesis tools,” *IEEE Transactions on Industrial Informatics*, vol. 14, no. 1, pp. 137–145, 2018.
- [17] T. A. Johansen, “Approximate explicit receding horizon control of constrained nonlinear systems,” *Automatica*, vol. 40, no. 2, pp. 293–300, 2004.
- [18] —, “On multi-parametric nonlinear programming and explicit nonlinear model predictive control,” in *IEEE Conference on Decision and Control*, vol. 3, 2002, pp. 2768–2773.
- [19] A. Bemporad, M. Morari, V. Dua, and E. N. Pistikopoulos, “The explicit linear quadratic regulator for constrained systems,” *Automatica*, vol. 38, no. 1, pp. 3 – 20, 2002.
- [20] T. Parisini and R. Zoppoli, “A receding-horizon regulator for nonlinear systems and a neural approximation,” *Automatica*, vol. 31, no. 10, pp. 1443–1451, 1995.

- [21] B. Karg and S. Lucia, “Efficient representation and approximation of model predictive control laws via deep learning,” *arXiv preprint arXiv:1806.10644*, 2018.
- [22] S. Chen, K. Saulnier, and N. Atanasov, “Approximating explicit model predictive control using constrained neural networks,” in *Proc. of the American Control Conference*, 2018, pp. 1520–1527.
- [23] I. Safran and O. Shamir, “Depth-width tradeoffs in approximating natural functions with neural networks,” in *Proceedings of the 34th International Conference on Machine Learning*, 2017, pp. 2979–2987.
- [24] M. Vidyasagar, *A Theory of Learning and Generalization*. London: Springer, 1997.
- [25] R. Tempo, G. Calafiore, and F. Dabbene, *Randomized Algorithms for Analysis and Control of Uncertain Systems, with Applications*, 2nd ed. London: Springer-Verlag, 2013.
- [26] S. Grammatico, X. Zhang, K. Margellos, P. Goulart, and J. Lygeros, “A scenario approach for non-convex control design,” *IEEE Transactions on Automatic Control*, vol. 61, no. 2, pp. 334–345, 2016.
- [27] M. Lorenzen, F. Dabbene, R. Tempo, and F. Allgöwer, “Stochastic MPC with offline uncertainty sampling,” *Automatica*, vol. 81, pp. 176–183, 2017.
- [28] M. Mammarella, M. Lorenzen, E. Capello, H. Park, F. Dabbene, G. Guglieri, M. Romano, and F. Allgöwer, “An offline-sampling SMPC framework with application to autonomous space maneuvers,” *IEEE Transactions on Control Systems Technology*, pp. 1–15, 2018.
- [29] G. Calafiore and M. Campi, “The scenario approach to robust control design,” *IEEE Transactions on Automatic Control*, vol. 51, no. 5, pp. 742–753, 2006.
- [30] L. Fagiano, M. Milanese, V. Razza, and I. Gerlero, “Control of power kites for naval propulsion,” in *Proc. of the American Control Conference*, 2010, pp. 4325–4330.
- [31] L. Deori, S. Garatti, and M. Prandini, “Trading performance for state constraint feasibility in stochastic constrained control: A randomized approach,” *Journal of the Franklin Institute*, vol. 354, no. 1, pp. 501–529, 2017.
- [32] K. Margellos, P. Goulart, and J. Lygeros, “On the road between robust optimization and the scenario approach for chance constrained optimization problems,” *IEEE Transactions on Automatic Control*, vol. 59, no. 8, pp. 2258–2263, 2014.
- [33] T. Alamo, R. Tempo, and E. Camacho, “Randomized strategies for probabilistic solutions of uncertain feasibility and optimization problems,” *IEEE Transactions on Automatic Control*, vol. 54, no. 11, pp. 2545–2559, 2009.
- [34] R. Tempo, E. Bai, and F. Dabbene, “Probabilistic robustness analysis: explicit bounds for the minimum number of samples,” *Systems & Control Letters*, vol. 30, pp. 237–242, 1997.
- [35] T. Alamo, R. Tempo, A. Luque, and D. Ramirez, “Randomized methods for design of uncertain systems: sample complexity and sequential algorithms,” *Automatica*, vol. 52, pp. 160–172, 2015.
- [36] M. Alamir, M. Fiacchini, I. Queinnec, S. Tarbouriech, and M. Mazerolles, “Feedback law with probabilistic certification for Propofol-based control of BIS during anesthesia,” *International Journal of Robust and Nonlinear Control*, vol. 28, no. 18, pp. 6254–6266, 2018.
- [37] M. Alamir, “On probabilistic certification of combined cancer therapies using strongly uncertain models,” *Journal of Theoretical Biology*, vol. 384, pp. 59–69, 2015.
- [38] M. Hertneck, J. Köhler, S. Trimpe, and F. Allgöwer, “Learning an approximate model predictive controller with guarantees,” *IEEE Control Systems Letters*, vol. 2, no. 3, pp. 543–548, 2018.
- [39] X. Zhang, M. Bujarbaruah, and F. Borrelli, “Safe and near-optimal policy learning for model predictive control using primal-dual neural networks,” *arXiv preprint arXiv:1906.08257*, 2019.
- [40] B. Karg and S. Lucia, “Learning-based approximation of robust nonlinear predictive control with state estimation applied to a towing kite,” in *Proc. of the European Control Conference*, 2019, pp. 16–22.

- [41] J. Rawlings and D. Mayne, *Model predictive control: Theory and design*. Nob Hill Pub., 2009.
- [42] M. Althoff and B. Krogh, “Reachability analysis of nonlinear differential-algebraic systems,” *IEEE Transactions on Automatic Control*, vol. 59, pp. 371–383, 2014.
- [43] A. Sahlodin and B. Chachuat, “Convex/concave relaxations of parametric ODEs using Taylor models,” *Computers & Chemical Engineering*, vol. 35, no. 5, pp. 844 – 857, 2011.
- [44] L. Hewing and M. N. Zeilinger, “Stochastic model predictive control for linear systems using probabilistic reachable sets,” in *2018 IEEE Conference on Decision and Control (CDC)*, 2018, pp. 5182–5188.
- [45] S. Subramanian, S. Lucia, and S. Engell, “A synergistic approach to robust output feedback control: Tube-based multi-stage NMPC,” *IFAC-PapersOnLine*, vol. 51, no. 18, pp. 500–505, 2018.
- [46] A. R. Barron, “Universal approximation bounds for superpositions of a sigmoidal function,” *IEEE Transactions on Information theory*, vol. 39, no. 3, pp. 930–945, 1993.
- [47] W. Hoeffding, “Probability inequalities for sums of bounded random variables,” *Journal of the American Statistical Association*, vol. 58, no. 301, pp. 13–30, 1963.
- [48] V. Blondel and J. Tsitsiklis, “A survey of computational complexity results in systems and control,” *Automatica*, vol. 36, no. 9, pp. 1249–1274, 2000.
- [49] M. Ahsanullah, V. Nevzorov, and M. Shakil, *An introduction to Order Statistics*. Paris: Atlantis Press, 2013.
- [50] B. Arnold, N. Balakrishnan, and H. Nagaraja, *A First Course in Order Statistics*. New York: John Wiley and Sons, 1992.
- [51] T. Alamo, J. Manzano, and E. Camacho, “Robust design through probabilistic maximization,” in *Uncertainty in Complex Networked Systems. In Honor of Roberto Tempo*, T. Basar, Ed. Birkhäuser, 2018, pp. 247–274.
- [52] T. Alamo, R. Tempo, and A. Luque, “On the sample complexity of randomized approaches to the analysis and design under uncertainty,” in *Proceedings of the American Control Conference*, Baltimore, USA, 2010.
- [53] B. Houska and M. Diehl, “Optimal control of towing kites,” in *Proc. of the 45th IEEE Conference on Decision and Control*, 2006, pp. 2693–2697.
- [54] L. Fagiano and C. Novara, “Automatic crosswind flight of tethered wings for airborne wind energy: a direct data-driven approach,” *IFAC Proceedings Volumes*, vol. 47, no. 3, pp. 4927–4932, 2014.
- [55] M. Erhard and H. Strauch, “Control of towing kites for seagoing vessels,” *IEEE Transactions on Control Systems Technology*, vol. 21, pp. 1629–1640, 2013.
- [56] S. Costello, G. François, and D. Bonvin, “Real-time optimization for kites,” in *Proc of the IFAC International Workshop on Periodic Control Systems (PSYCO)*, 2013, pp. 64–69.
- [57] S. Costello, G. François, and D. Bonvin, “Crosswind kite control—a benchmark problem for advanced control and dynamic optimization,” *European Journal of Control*, vol. 35, pp. 1–10, 2017.
- [58] F. Chollet *et al.*, “Keras,” <https://github.com/fchollet/keras>, 2015.
- [59] M. A. et al., “TensorFlow: Large-scale machine learning on heterogeneous systems,” 2015, software available from tensorflow.org. [Online]. Available: <http://tensorflow.org/>
- [60] D. P. Kingma and J. Ba, “Adam: A method for stochastic optimization,” *CoRR*, vol. abs/1412.6980, 2014.

AUTHOR BIOGRAPHY

Benjamin Karg, was born in Burglengenfeld, Germany, in 1992. He received the B.Eng. degree in mechanical engineering from Ostbayerische Technische Hochschule Regensburg, Regensburg, Bavaria, Germany, in 2015, and his M.Sc. degree in systems engineering and engineering cybernetics from Otto-von-Guericke Universität, Magdeburg, Saxony-Anhalt, Germany, in 2017. He currently works as a research assistant at the laboratory "Internet of Things for Smart Buildings", Technische Universität Berlin, Germany, to pursue his PhD. He is also member of the Einstein Center for Digital Future.

His research is focused on control engineering, artificial intelligence and edge computing for IoT-enabled cyber-physical systems.



Teodoro Alamo was born in Spain in 1968. He received the M.Eng. degree in telecommunications engineering from the Polytechnic University of Madrid, Spain, in 1993 and the Ph.D. degree in telecommunications engineering from the University of Seville, Spain, in 1998. From 1993 to 2000, he was an Assistant Professor, an Associate Professor from 2001 to 2010, and has been a Full Professor since March 2010 with the Department of System Engineering and Automatic Control, University of Seville. He was at the Ecole Nationale Supérieure des Telecommunications (Telecom Paris) from September 1991 to May 1993. Part of his Ph.D. was done at RWTH Aachen, Germany, from June to September 1995.

He is the author or coauthor of more than 200 publications including books, book chapters, journal papers, conference proceedings, and educational books. (google scholar profile available at <http://scholar.google.es/citations?user=W3ZDTkIAAAAJ&hl=en>). He has co-funded the spin-off company Optimal Performance (University of Seville, Spain). His current research interests include decision making, model predictive control, machine learning, randomized algorithms, and optimization strategies..



Sergio Lucia, received the M.Sc. degree in electrical engineering from the University of Zaragoza, Zaragoza, Spain, in 2010, and the Dr. Ing. degree in optimization and automatic control from the Technical University of Dortmund, Dortmund, Germany, in 2014. He joined the Otto-von-Guericke Universität Magdeburg and visited the Massachusetts Institute of Technology as a Postdoctoral Fellow.

Since May 2017, he has been an Assistant Professor and Chair with the Laboratory of Internet of Things for Smart Buildings, Technische Universität Berlin, Berlin, Germany, and with Einstein Center Digital Future, Berlin. His research interests include decision-making under uncertainty, distributed control, as well as the interplay between machine learning techniques and control theory. Dr. Lucia is currently Associate Editor of the Journal of Process Control.

